Identification of Gas Phase PAHs in Absorption Towards Protostellar Sources[1]

Jesse D. Bregman
Astrophysics Branch, NASA-Ames Research Center

Pasquale Temi
Astrophysics Branch, NASA-Ames Research Center and SETI Institute

Received ________________________; accepted ________________________

---

[1] Based on observations with ISO, an ESA project with instruments funded by ESA Member States (especially the PI countries: France, Germany, the Netherlands and the United Kingdom) and with the participation of ISAS and NASA.

1. Introduction

The infrared emission bands (also known as the UIR bands) have recently been observed in absorption at 3.25 μm in the ices surrounding a few proto-stellar objects (Sellgren et al. 1994, 1995; Brooke, Sellgren, and Smith 1996; Brooke, Sellgren, and Geballe 1999), at 11.2 μm in MonR2 (Bregman, Hayward, and Sloan 2000), and at 6.2 μm towards two sources near the galactic center (Schutte et al. 1998). The UIR bands have been observed in emission for many years, but identifying these bands has proven to be both difficult and contentious as no one has yet found a single material that provides a good match to the features. However, most investigators agree that some form of carbon-based material with aromatic bonds is the most likely candidate, and many arguments favor free molecules (polycyclic aromatic hydrocarbons, PAHs) as the carriers of at least the narrow emission bands. Since the emission arises not from a single molecule but from a family of molecules, identifying which PAHs are contributing to the infrared emission bands is difficult. The identification is further complicated by the fact that the emission at short wavelengths is dominated by small molecules while at long wavelengths it is dominated by large molecules (Schutte, Tielens, and Allamandola 1993). Thus, for example, the emission at 3.3 μm is from a different mix of molecules than those which produce the 11.2 μm band. To complicate matters further, the molecular mix includes both neutral and ionic species. In absorption, the same mixture of molecules contributes at all wavelengths and the molecules should be neutral, potentially simplifying comparisons with lab data. Also, absorption strengths measured in the lab are directly applicable to interstellar absorption bands without the need to model an emission spectrum of an unknown mixture of ionized and neutral PAHs.

In this paper we show that a mixture of argon matrix isolated PAH molecules can reproduce the 3.25 μm absorption band seen in the ISO SWS spectrua of four embedded infrared sources, S140 IRS1, AFGL 2591, Elias 29, and AFGL 989. In section 2 we describe the ISO SWS data analysis and in section 3 discuss the results.

2. Data Analysis

All of the sources have been observed with the Short Wavelength Spectrometer (SWS) (de Graauw et al. 1996) on-board the Infrared Space Observatory (ISO) (Kessler et al. 1996) satellite. Two different data sets were available from the ISO DATA Archive, both using the AOT1 scanning mode, covering the entire 2.4-45.2 μm SWS wavelength range. We present data taken at "speed 4" corresponding to a resolution $\lambda/\Delta\lambda$=1400. Data have been reduced using both the Observer SWS Interactive Analysis (OSIA) and the

PAH absorption feature and seems unrealistic based on the band position in S140, where there is little uncertainty about the continuum. However, the rather broad 3.25 μm absorption in Elias 29 makes it more difficult to define the continuum than in the other sources.

3. Discussion

3.1. Spectral Fits

The comparisons shown in Figure 3 demonstrate that laboratory absorption spectra of isolated PAHs can fit the spectra quite well. No single PAH has a broad enough absorption band to fit the entire 3.25 μm absorption feature, with band widths ranging from 0.015 to 0.035 μm FWHM for laboratory matrix isolated PAHs compared to these sources which have widths from 0.059 to 0.093 μm. The fits shown in Fig. 3 are not unique, as shown by the two fits for S140. In the top S140 spectrum, three PAHs were used to fit the data (hexabenzocoronene A, benzo[b]fluoranthene, and anthracene), while in bottom spectrum (labeled fit 2), only two were used (triphenylene and chrysene). Similarly, the other spectra can be fitted with various PAH mixtures. However, even though the fits are not unique, there are some general spectral properties apparent from the twenty PAH spectra published by Hudgins and Sandford. In these PAHs, which are obtained in an Ar ice matrix to simulate isolated molecules, fifteen show an absorption feature near 3.265 μm while only two have a band at 3.24 μm. Thus, it appears that absorption at 3.265 μm is a general property of many different isolated PAHs. The two molecules that have an absorption band at 3.24 μm have similar geometries, with complete rings alternating with missing rings arranged symmetrically on the periphery of the molecule (triphenylene looks like a little propeller, with one central ring and three surrounding rings). While the comparison between the lab data and these sources is quite good, and the 3.265 μm absorption is a general property of small PAHs, we should keep in mind that the laboratory database has only a limited number of PAH spectra, and contains spectra of only two PAHs with more than 20 carbon atoms. There have been many arguments that PAHs with fewer than about 24 carbon atoms would not survive in the UV field encountered in planetary nebulae, HII regions, and the interstellar medium (ISM). Thus, the laboratory PAH sample represents, at best, the smallest PAHs thought to exist in the ISM. The match of the protostar data with laboratory spectra of isolated PAHs is surprising since the PAHs are associated with a strong water ice absorption, and therefore would most likely be contained in the water ice matrix if the water and PAHs were co-deposited from the gas phase. PAH molecules both in the solid phase in high enough concentrations in water ice to be visible, interact with neighboring PAH

The intrinsic band strengths of the C-H stretch in PAHs varies among the different molecules by about a factor of two (Hudgins and Sandford 1998a, 1998b; Joblin et al. 1994). For the C-H stretch in coronene, Joblin et al. (1994) get a value of 2.2x10-18 cm/C-H bond in the gas phase and a value 3.3 times smaller for solid coronene. The solid coronene value is the same as that measured by Leger et al. (1989) for coronene dispersed in a KBr pellet. Hudgins and Sandford (1998a) measure the relative strengths of the coronene bands and compare them to theoretical calculations of gas phase PAHs from Langhoff (1996) who gives absolute intensities. However, Hudgins and Sandford note that the theoretical values for the C-H stretching region are generally too large by about a factor of two. Taking this factor into account results in a value of 2.0x10-18 cm/C-H bond, in good agreement with the value given by Joblin et al. While the PAH mixture certainly contains molecules other than coronene, coronene is one of the few large PAH molecules measured in the lab, and its integrated C-H stretch intensity is similar to other large PAHs. Joblin et al. (1994) also point out that the intensity of the C-H stretch from solo hydrogens, those with no adjacent hydrogen atom on the periphery of the PAH molecule, are 3.5 times stronger than non-solo hydrogen stretches. Bregman, Hayward, and Sloan (2000) estimate that about 25% of the PAHs along the line-of-sight to MonR2 IRS1 are solo hydrogens. Thus, we adopt an intrinsic C-H stretch intensity for the PAH mix of 3.6x10-18 cm per C-H bond. This is somewhat larger than the value adopted by Sellgren et al. (1995) since they averaged values for both solid phase and gas phase PAHs. Since we have evidence that the PAHs are in the gas phase, we prefer the larger value, which results in the values listed in the second column of Table 2. If the PAHs are in the solid phase, then the column densities and carbon fractions listed in Table 2 should be increased by a factor of 3.3, resulting in a rather large fraction of the available carbon tied up in PAHs in Elias 29 (89%) and GL989 (30%). For the aliphatic molecules, we adopt the value given by Allamandola et al. (1992) of 4x10-18 cm per C-H. Since the column densities listed in Table 2 are the number of C-H bonds along the line-of-sight, we have to know the number of carbon atoms per C-H bond to calculate the fraction of available carbon tied up in both PAHs and aliphatics along with the hydrogen column density and the cosmic abundance of carbon. We can estimate the number of carbon atoms per C-H bond for PAHs by assuming that coronene is the smallest PAH likely to survive in the ISM. Coronene has a C/H ratio of 2, while larger molecules have larger C/H ratios. Since the most stable PAHs are condensed molecules, we expect that the average PAH will have a C/H ratio between 2 and 3, and so adopt a ratio of 2.5. Aliphatic molecules are long chains, and saturated aliphatics approach a C/H ratio of 0.5. The hydrogen column density can be calculated from the silicate optical depth by assuming a ratio for Av/t(9.7) and for NH/Av. For these calculations, we adopt NH/Av=1.9x10-21 cm-2 (Bohlin et al. 1978), and Av/t(9.7)=18.9 (Roche and Aitken 1984; Whittet et al. 1997), the value measured for the diffuse ISM. However, Av/t(9.7) varies

We wish to thank the staff at IPAC for their help with understanding how to analyze the ISO data.

REFERENCES

Allamandola, L.J., Sandford, S., Tielens, A.G.G.M., and Herbst, T.M. 1992, ApJ, 399, 134.

Boogert, A.C.A. et al. 2000, A&A, 360, 683.

Bregman, J.D., Hayward, T., and Sloan, G. 2000, ApJ, submitted.

Brooke, T.Y., Sellgren, K., and Smith, R.G. 1996, ApJ, 459, 209.

Brooke, T.Y., Sellgren, K., and Geballe, T.R. 1999, ApJ, 517, 883.

de Graauw et al. 1996, A&A, 315, L49

Gillett, F.C., Jones, T.W., Merrill, K.M., and Stein, W.A. 1975, A&A, 45, 77.

Harker, D., Bregman, J., Tielens, A.G.G.M., Temi, P., and Rank, D. 1997, A&A, 324, 629.

Harvey, P.M., Campbell, M.F., and Hoffman, W.F. 1978, ApJ, 219, 891.

Hudgins, D.M, and Sandford, S.A. 1998a, J.Phys.Chem., 102, 329.

Hudgins, D.M, and Sandford, S.A.1998b, J.Phys.Chem., 102, 344.

Hudgins, D.M, and Sandford, S.A.1998c, J.Phys.Chem., 102, 353.

Kessler, M.F. et al 1996, A&A315, L27

Merrill, K.M., Russell, R.W., and Soifer, B.T. 1976, ApJ, 207, 763.

Papoular, R., Conard, J., Guillois, O., Nenner, I., Reynaud, C., and Rouzaud, J.-N. 1996, A&A, 315, 222.

Schutte, W.A. et al. 1998, A&A, 337, 261.

Schutte, W.A., Tielens, A.G.G.M., and Allamandola,L.J. 1993, ApJ, 415, 397.

Scott, A., and Duley, W.W. 1996, ApJ, 472, L123.

Sellgren, K., Smith, R.G., and Brooke, T.Y. 1994, ApJ, 433, 179.

Sellgren, K., Brooke, T.Y., Smith, R.G., and Geballe, T.R. 1995, ApJ, 449, L69.

Willner, S.P. et al. 1982, ApJ, 253, 174.

Wilner, D.J., and Welch, W.J. 1994, ApJ, 427, 898.

This manuscript was prepared with the AAS LaTeX macros v4.0.

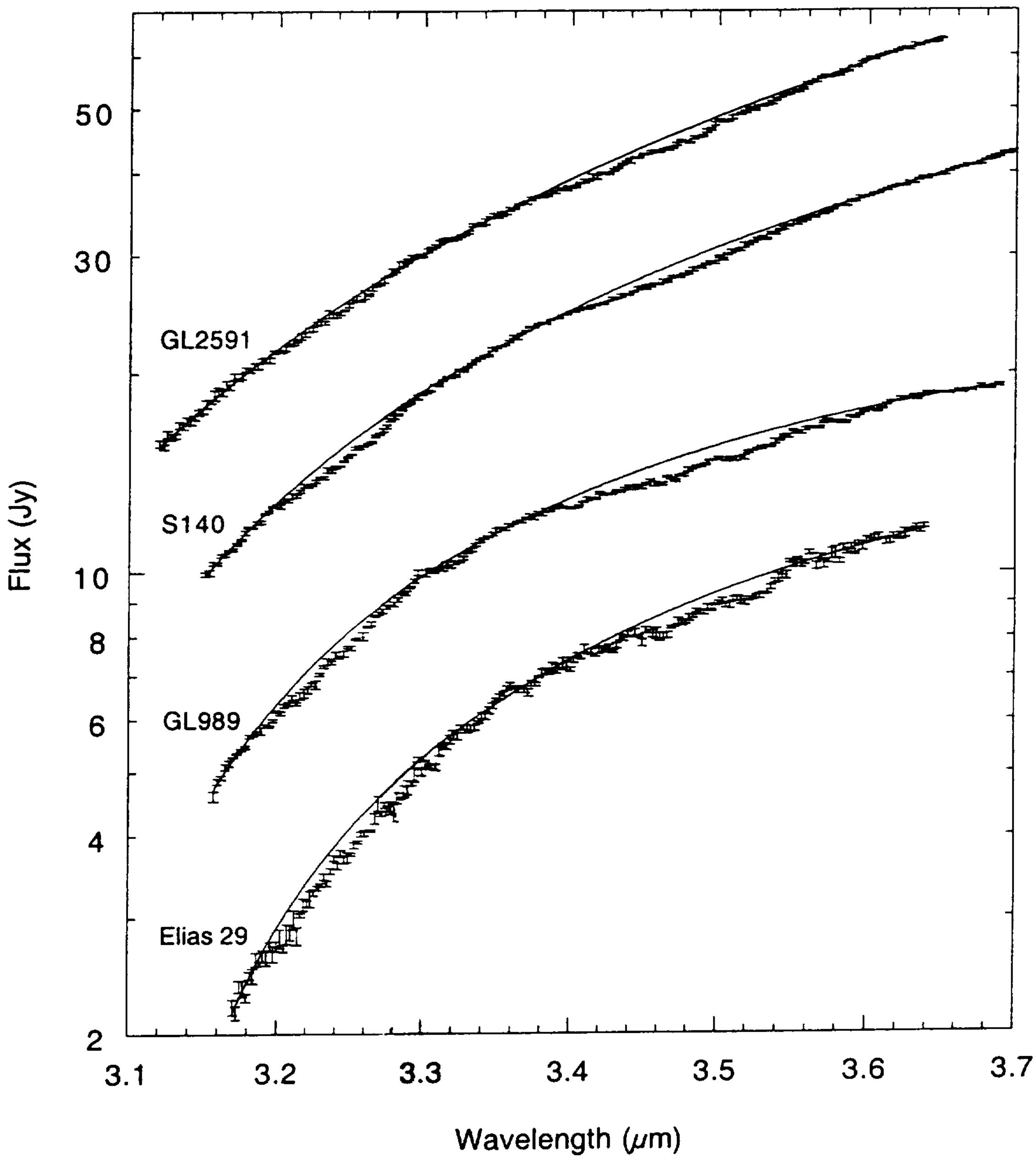

GL2591
S140
GL989
Elias 29
Flux (Jy)
50
30
10
8
6
4
2
3.1
3.2
3.3
3.4
3.5
3.6
3.7
Wavelength (μm)

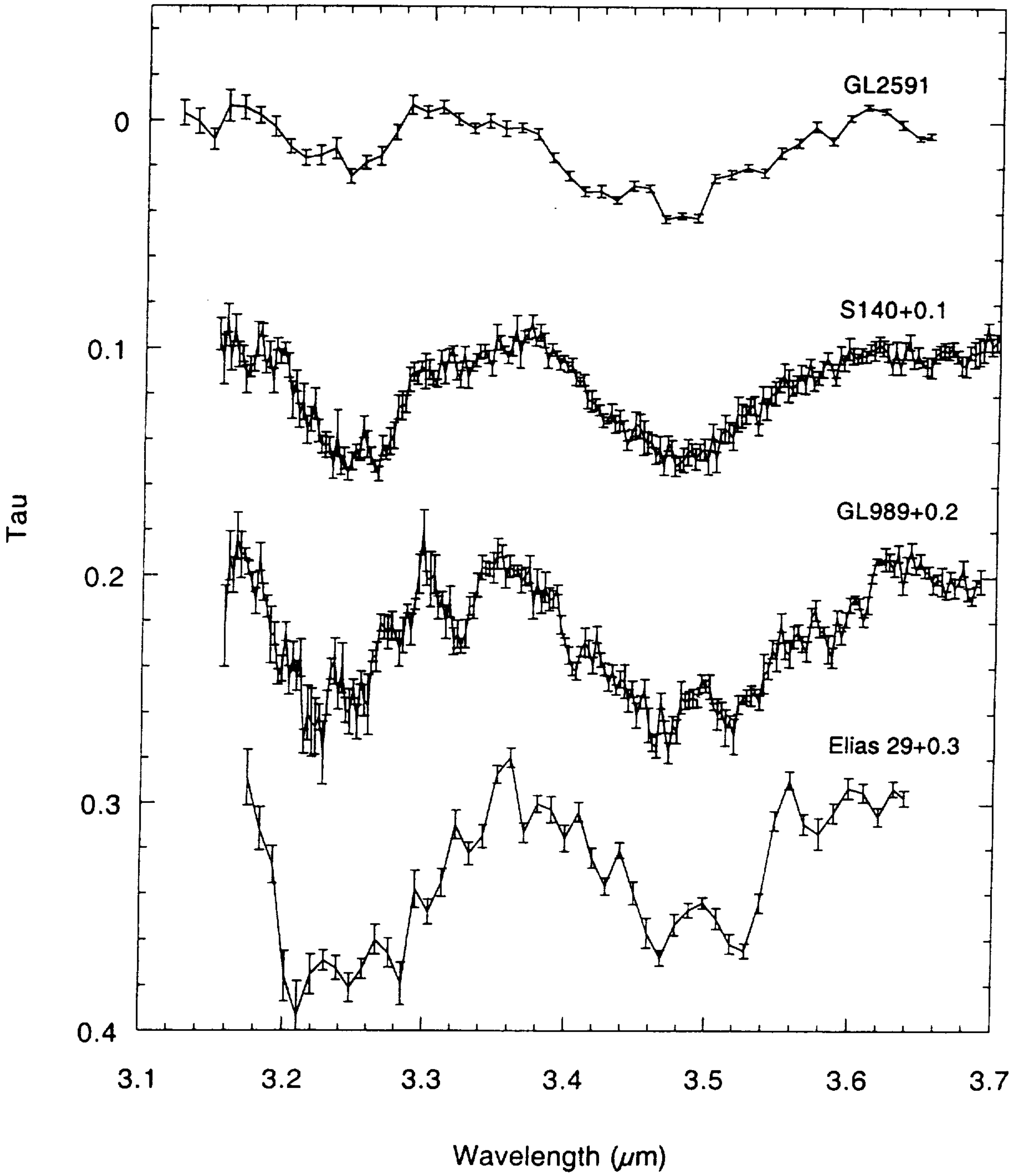
GL2591
S140+0.1
GL989+0.2
Elias 29+0.3
Tau
0
0.1
0.2
0.3
0.4
3.1
3.2
3.3
3.4
3.5
3.6
3.7
Wavelength (μm)

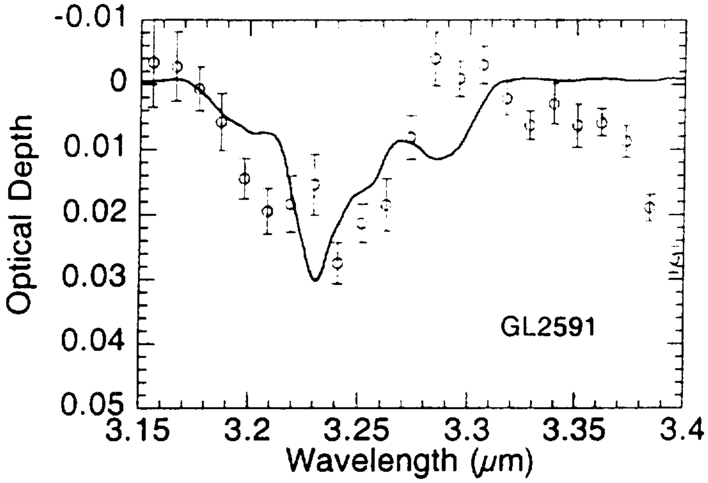
GL2591
Optical Depth
Wavelength (μm)
-0.01
0
0.01
0.02
0.03
0.04
0.05
3.15
3.2
3.25
3.3
3.35
3.4

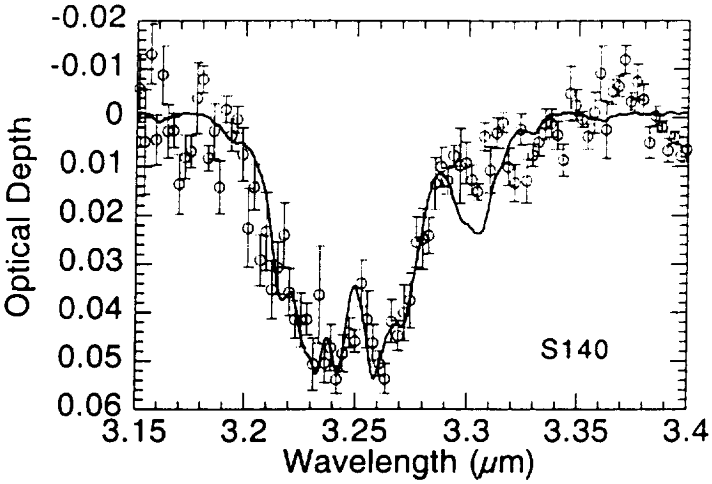
S140
Optical Depth
Wavelength (μm)
-0.02
-0.01
0
0.01
0.02
0.03
0.04
0.05
0.06
3.15
3.2
3.25
3.3
3.35
3.4

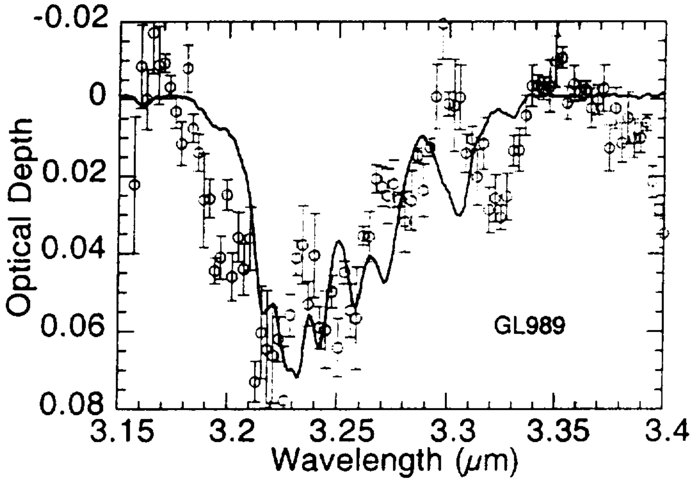
GL989
Optical Depth
Wavelength (μm)
-0.02
0
0.02
0.04
0.06
0.08
3.15
3.2
3.25
3.3
3.35
3.4

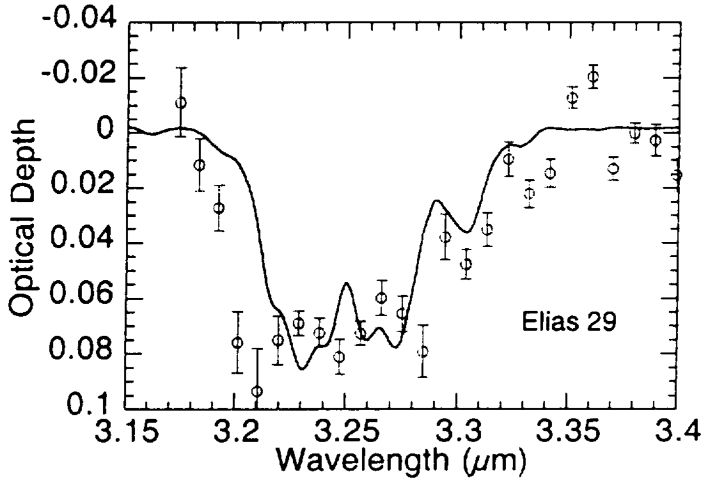
Elias 29
Optical Depth
Wavelength (μm)
-0.04
-0.02
0
0.02
0.04
0.06
0.08
0.1
3.15
3.2
3.25
3.3
3.35
3.4

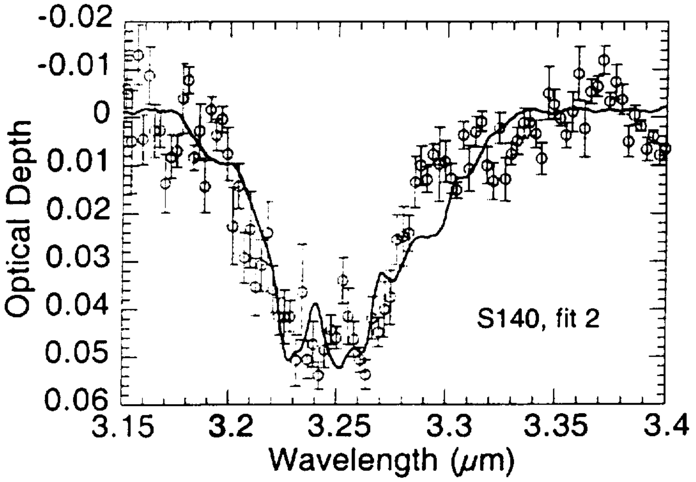
S140, fit 2
Optical Depth
Wavelength (μm)
-0.02
-0.01
0
0.01
0.02
0.03
0.04
0.05
0.06
3.15
3.2
3.25
3.3
3.35
3.4